

Received June 10, 2020, accepted June 16, 2020, date of publication June 19, 2020, date of current version July 1, 2020.

Digital Object Identifier 10.1109/ACCESS.2020.3003698

Experimental Validation of a 2-Bit Reconfigurable Unit-Cell for Transmitarrays at Ka-Band

ANTONIO CLEMENTE^{1,2}, (Senior Member, IEEE),
FATIMATA DIABY^{1,2}, LUCA DI PALMA^{1,2}, (Member, IEEE),
LAURENT DUSSOPT^{1,2}, (Senior Member, IEEE),
AND RONAN SAULEAU^{1,2,3}, (Fellow, IEEE)

¹ Université Grenoble-Alpes, 38400 Grenoble, France

² CEA-Leti, 38054 Grenoble, France

³ CNRS, Institut d'Électronique et de Télécommunications de Rennes (IETR), University of Rennes 1, 35000 Rennes, France

Corresponding author: Antonio Clemente (antonio.clemente@cea.fr)

This work was supported by the National Research Agency through the project TRANSMIL under Grant ANR-14-CE28-0023.

ABSTRACT This paper presents the experimental results of a 2-bit electronically reconfigurable unit-cell for transmitarrays at Ka-band. The proposed unit-cell architecture is based on a six-metal layers design and three dielectric substrates. Two patch antennas are printed respectively on the top and bottom layers of the stack-up to achieve an antenna-filter-antenna structure. To implement the desired 2-bit phase resolution, two p-i-n diodes are bonded on each patch. The unit-cell has been fabricated and characterized in a specific waveguide simulator. The measurement results are compared to the simulated ones and show minimum transmission loss in the range 1.5 – 2.3 dB. The 3-dB fractional bandwidth is in the range 10.1 – 12.1%.

INDEX TERMS Transmitarray antennas, beam steering, beam forming, Ka-band, discrete lens, electronically steerable antenna.

I. INTRODUCTION

Relatively low cost and low power consumption beam-forming architectures are required to develop innovative electronically steerable antennas for the future mass market high-data-rate satellite and terrestrial communications. In this context, spatial feeding techniques combined with Printed Circuit Boards (PCB) technologies represent cost-effective solutions to design innovative electronically reconfigurable antennas based on the reflectarray or transmitarray concepts [1]. On one side, for large antenna apertures, the spatial feeding mechanism drastically reduces the loss and complexity of the power division network compared to classical phased array architectures. On the other side, PCB technologies are compatible with the integration on the array aperture of p-i-n diodes, RF-MEMS switches, varactors, etc., which can be used to easily control the antenna aperture phase distribution without using complex and lossy phase shifters. Furthermore, as they operate in transmission mode, transmitarrays are also compatible with solutions to reduce the overall antenna profile [2]–[4].

Several printed electronically steerable transmitarrays have been demonstrated in the last decade from L- up

The associate editor coordinating the review of this manuscript and approving it for publication was Guido Valerio¹.

to Ka-band [5]. Continuous phase control [6]–[8] or phase quantization techniques [9]–[16] are used to tune the transmission phase and perform beam-forming functions.

This paper focuses on the experimental characterization of a 2-bit unit-cell based on p-i-n diodes and operating at Ka-band. Therefore, this unit-cell can be electronically reconfigured to provide four phase states mutually shifted by 90°. A 2-bit phase quantization significantly improves the transmitarray performance in terms of collimating capability (e.g. improved directivity and lower side lobe level) compared to the 1-bit architectures. At same time, such an approach provides a very good trade-off between number of solid-state components, complexity of the bias network, efficiency, bandwidth, and power consumption, compared to the continuous phase shift based unit-cell designs. Indeed, a transmitarray with a 2-bit phase quantization exhibits a typical aperture efficiency around 30-40% [15], [16], which is comparable to configurations with continuous phase control [2].

To the best of the authors' knowledge, excluding our very preliminary studies [17], only one 2-bit electronically reconfigurable unit-cell based on RF-MEMS switches has been previously demonstrated [9]. However, such unit-cell has been realized considering a wafer-based technology and

includes five switches biased with six independent bias lines. This solution is much more complex than the one proposed here where we use only four p-i-n diodes and two bias lines per unit-cell. Furthermore, the performance presented in [9] are highly affected by the large value of the RF-MEMS switch resistance, with insertion loss in the range 4.9-9.2 dB (depending on the phase-shift state of the unit-cell). As clearly presented in the recent survey paper [5], phase quantization with 1-bit resolution is typically used in the actual state-of-the-art on electronically reconfigurable transmitarrays; this choice is often driven by the fact that 1-bit phase quantization can be achieved using a limited number of switches and metal layers. The unit-cell architecture validated experimentally here paves the way for 2-bit steerable transmitarrays at Ka-band, with improved performance compared to their 1-bit counterparts.

This paper is organized as follows. The fabricated 2-bit unit-cell and its experimental setup in waveguide are presented in Section II. The measurement results are discussed in Section III. They are also compared to those achieved with full-wave electromagnetic simulations. Moreover, the impact of the bias current is also discussed. Finally, conclusions are drawn in Section IV.

II. 2-BIT RECONFIGURABLE UNIT-CELL: FABRICATION AND EXPERIMENTAL SETUP

A. FABRICATED UNIT-CELL

The proposed unit-cell (size of $5.1 \times 5.1 \times 1.3 \text{ mm}^3$, $\lambda_0/2 \times \lambda_0/2 \times \lambda_0/8$ at 29 GHz) has been recently used to demonstrate an electronically reconfigurable transmitarray showing the possibility to steer the beam over a 120×120 -degree window [15], [16]. Nonetheless, its individual characterization has never been reported yet. This constitutes the main objective of this contribution.

The proposed architecture is based on six-metal layer (M1 – M6 in Fig. 1(a), thickness $18 \mu\text{m}$) stack-up with three RT/Duroid 6002 Rogers substrates ($\epsilon_r = 2.94$, $\tan\delta = 0.0012$) and two bonding films (RO4405F, $\epsilon_r = 3.52$, $\tan\delta = 0.004$, thickness $100 \mu\text{m}$). The substrate between layers M5-M6 has a thickness of $508 \mu\text{m}$. Instead, the substrates between layers M1-M2 and M3-M4 have a thickness of $254 \mu\text{m}$. The six metal layers are the following: transmitting (Tx) patch antenna (M1), delay line (M2), bias line associated to the Tx patch (M3), ground plane (M4), bias line associated to the receiving (Rx) patch (M5), and the Rx patch (M6). Standard Printed Circuit Board (PCB) process, *i.e.* with minimum trace width of $80 \mu\text{m}$ and minimum via-diameter of $120 \mu\text{m}$, has been selected to demonstrate the possibility to implement the proposed design by using mature and relatively low cost fabrication technologies.

Two p-i-n diodes MACOM MA4AGP907, indicated as D1 – D4 in Fig. 1, are flip-chipped on each radiating element (O-slotted rectangular patch antennas, as represented in Fig. 1(b)) to control electronically the transmission phase of the unit-cell with the required 2-bit phase resolution. Four phase states (UC000, UC090, UC180, and UC270)

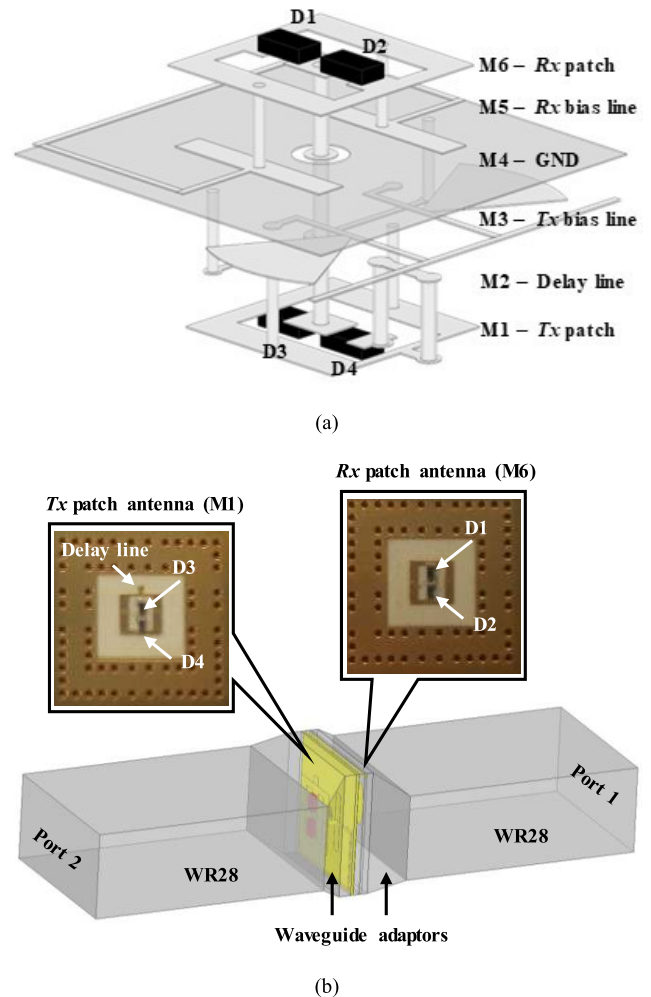


FIGURE 1. Reconfigurable 2-bit unit-cell. (a) Three-dimensional view. (b) Schematic view of the experimental setup (waveguide simulator) and photographs of the realized prototype: transmitting (Tx) patch printed on metal layer M1, and receiving (Rx) patch printed on M6.

are generated by opportunely controlling the diode states as presented in Table 1.

The two patch antennas having an O-slot are connected by a metallized via hole, with a diameter of $200 \mu\text{m}$, to implement an Antenna-Filter-Antenna unit-cell. For isolation reason, a $700\text{-}\mu\text{m}$ diameter hole is realized in the ground plane to allow the passage of this via. Metallized vias of diameter $150 \mu\text{m}$ are realized between M1-M2, M3-M4, and M5-M6 to correctly bias the p-i-n diodes and realize the 90° delay line connected on the Tx-patch.

From Table 1 it is clear that four switches (*i.e.* p-i-n diodes in this specific design) is the minimum number of devices required to achieve a 2-bit phase quantization. The number of diodes per unit-cell used in our design can be compared with ref. [9] where 5 RF-MEMS switches are used to achieve the same phase resolution. Furthermore as both diodes of each pair of p-i-n diodes (*i.e.* D1-D2 and D3-D4) are biased in opposite state (see Fig. 2(a)), the proposed unit-cell contains only two bias lines, as compared to 6 lines required [9].

TABLE 1. P-i-n diodes bias state as a function of the unit-cell transmission phase state.

Unit-Cell	D1	D2	D3	D4
UC000	ON	OFF	ON	OFF
UC090	ON	OFF	OFF	ON
UC180	OFF	ON	ON	OFF
UC270	OFF	ON	OFF	ON

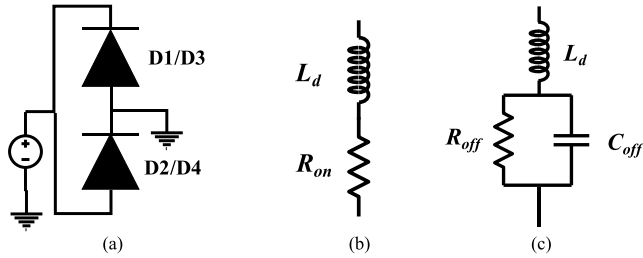


FIGURE 2. (a) Configuration of the p-i-n diodes mounted in the opposite direction (series). Equivalent model of the diode p-i-n: (b) forward bias (ON), and (c) reverse bias (OFF).

The equivalent electrical model of the diodes (see Fig.s 2(b)-(c)) has been extracted up to 40 GHz by fitting, in simulations, two-port on-probe measured S-parameters of the devices mounted on an *ad-hoc* board [18]. For a forward bias current I_{bias} equal to 10 mA, the equivalent model consists of a series L-R circuit ($R_{on} = 4.2 \Omega$ and $L_d = 0.05$ nH). In the reverse state ($V_{bias} = 1.2$ V), the diode is modelled as a shunt R-C circuit ($R_{off} = 300$ k Ω and $C_{off} = 42$ fF) with a series inductor ($L_d = 0.05$ nH). The Gallium-Arsenide packaging ($\epsilon_r = 12.9$) of the p-i-n diodes, with dimensions of $0.686 \times 0.368 \times 0.19$ mm³, is also included in the full-wave model of the unit-cell (see Fig. 1(a)). More details on the unit-cell optimization, full-wave simulation

setup, geometrical parameters, and operation principle are presented in our preliminary paper [17].

The unit-cell operation principle and p-i-n diode impacts can be analyzed by plotting the surface current distributions computed on the Tx and Rx patch antennas as a function of the diode states (Fig. 3). As presented in Fig. 3(a) and considering the configuration of Fig. 2(a), when the Tx patch is biased with a positive current D1 is ON, whereas D2 is in the OFF state. By inverting the sign of the bias current (D1 OFF and D2 ON, Fig. 3(b)), the current flow is inverted and a phase-shift of 180° is achieved. Almost the same behavior is achieved on the Rx patch when the diodes D3 and D4 are controlled (Fig.s 3(c)-(d)). However, when the diodes D3 is ON and D4 is OFF (Fig. 3(d)), the current flows on the delay line producing a 90° phase-shift.

B. ELECTROMAGNETIC SIMULATION AND MEASUREMENT SETUPS

The unit-cell has been characterized using a waveguide simulator based on standard WR28 waveguides (7.112×3.556 mm²), as presented in Fig. 1(b). It is composed by two coax-to-WR28 adaptors, two WR28 straight waveguide sections, and two tapered transitions between the rectangular section of the waveguide and the square aperture of the unit-cell. The length of these transitions equals 1.2 mm ($\lambda/8.6$); its value has been optimized to minimize the impedance mismatch and the impact of oblique incidence in the waveguide simulator [19].

Full-wave simulations using Ansys HFSS v2019 have been performed to study the impact of oblique incidence on the scattering parameters of the unit-cell. For this purpose, three different configurations have been considered: unit-cell embedded in a WR28 standard rectangular waveguide (Fig. 1(b)), unit-cell with periodic boundary conditions

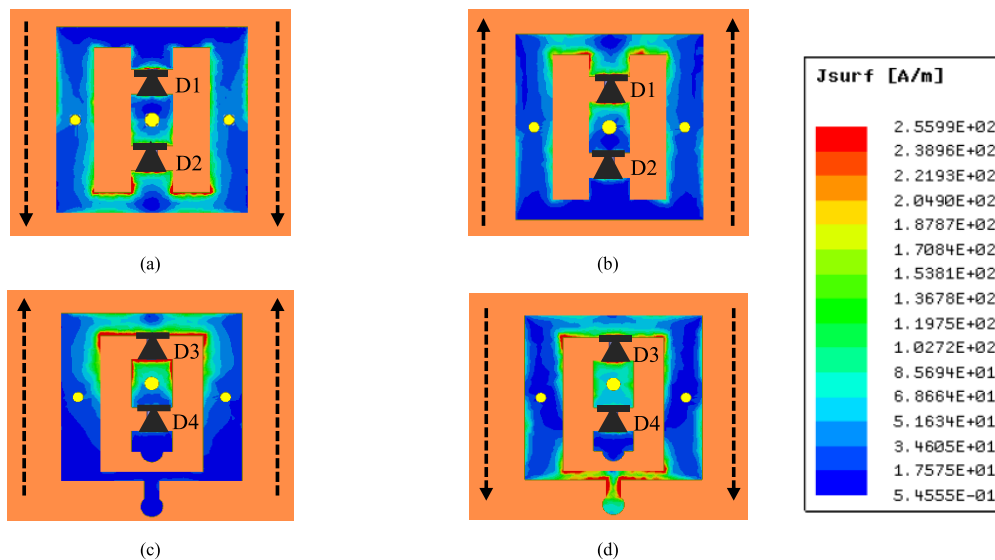


FIGURE 3. Surface current distributions of the unit-cell for the four phase states on the Tx and Rx patch antennas. (a) Tx patch when D1 is ON and D2 is OFF, (b) Tx patch when D1 is OFF and D2 is ON, (c) Rx patch when D3 is ON and D4 is OFF, and (d) Rx patch when D3 is OFF and D4 is ON.

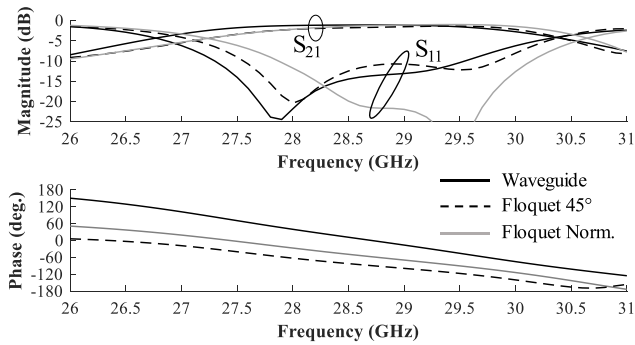


FIGURE 4. Magnitude and phase of the reflection and transmission coefficients of the phase state UC000. Simulations in waveguide, and with Floquet ports for normal incidence and 45° oblique incidence.

and Floquet ports, for normal incidence and for 45° oblique incidence. The 45° incidence has been selected as it coincides with the equivalent incidence angle of the fundamental TE₁₀ mode in the WR28 waveguide at 29 GHz. Furthermore, 45° is close to the maximum incidence angle for a transmitarray with a typical focal over aperture size (F/D) ratio in the range 0.5 – 0.7.

Here, for brevity reasons, we compare the three simulation setups (e.g. Waveguide, Floquet 45°, and Floquet Norm.) only for the 0° phase state (UC000, Fig. 4). The conclusion of this analysis is similar to the case of the 1-bit unit-cell (see [18]) and shows that, there are slight differences between the magnitude of the simulated scattering parameters computed with 45° oblique incidence and with the full waveguide setup. A frequency shift around 500 MHz is obtained in reflection (S_{11}) between the results in waveguide and under normal incidence. Moreover, there is a phase difference up to 80° in the 27 – 30 GHz frequency range when comparing the transmission phase computed with the waveguide setup and with the Floquet boundary conditions under normal incidence. In the same frequency band, the phase difference between the Floquet simulations under normal and 45° incidence is lower than 40°. The phase variation achieved with the waveguide setup is mostly due to the presence of the rectangular-to-square waveguide transition, which is not de-embedded as in the case of the calibration process used in the measurements. Note that in the rest of the paper, the measurement results are compared to the simulations including the full waveguide experimental setup.

III. EXPERIMENTAL CHARACTERIZATION

We compare here the experimental results of the unit-cell obtained with the measurement setup described in Section II.B and with 3D full-wave simulations. The impact of the bias lines on the unit-cell performance has been also analyzed; for brevity purposes, we only consider the unit-cell with two bias lines, one for each pair of p-i-n diodes. The complete study considering a 14 × 14-element transmitarray is presented in [15]. The obtained results show very stable scattering parameters, demonstrating that the bias lines do not affect the RF performance.

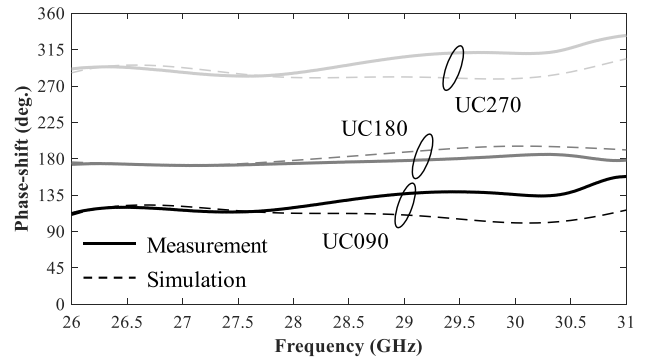


FIGURE 5. Simulated and measured relative phase-shifts between the UC000 and the other phase states.

A. SCATTERING PARAMETERS

The results presented in this section have been obtained by considering a p-i-n diode forward bias current of ± 10 mA. The simulated and measured relative phase-shifts between the UC000 and the other phase states are plotted in Fig. 5. The phase values measured between 27 and 30.2 GHz vary in the ranges 114.2°-138.3°, 172.3°-185.4°, and 282.4°-311.6°, for the phase states UC090, UC180, and UC270, respectively. They are in acceptable agreement with the simulation data (the corresponding phase-shift ranges equal 100.8°-121.2°, 172.2°-195.6°, and 279.3°-292.9°, respectively).

The measured and computed reflection and transmission coefficients are plotted in Fig. 6 in amplitude for the four phase states. The simulated 3-dB fractional transmission bandwidth (BW) is equal to 9.6%, 16.5%, 12.1% and 15.5% for UC000, UC090, UC180, and UC270, respectively. These values are in acceptable agreement with the measured ones (11.7%, 10.1%, 12.1%, and 10.3%, respectively). Furthermore, the measured insertion loss at 29 GHz equals 2.1, 1.5, 2.3, and 1.6 dB for the UC000, UC090, UC180, and UC270, respectively. Also in this case they are in acceptable agreement with the simulated data (1.0, 0.8, 1.0, and 0.8 dB, respectively).

The discrepancies observed between measurements and simulations are probably due to the fabrication tolerances of the six-metal-layer PCB, including layer misalignments (*i.e.* ± 50 μm), unit-cell geometrical dimensions (*i.e.* ± 30 μm for the trace width and length, ± 50 μm for the via diameters), non-uniform thickness of the bonding film layers due to the bonding process (*i.e.* up to 30 μm less than the nominal value), etc., and to the misalignment of the unit-cell in the waveguide setup. However, the systematic analysis of possible manufacturing errors cannot be easily performed due to the large number of design parameters. Despite the observed differences between measurements and simulations in terms of insertion losses and -10 dB reflection bandwidth, the working principle of the active unit-cell has been validated. Furthermore, the non-perfect 90° phase-shift does not affect the overall performance of the transmitarray, as demonstrated in [15].

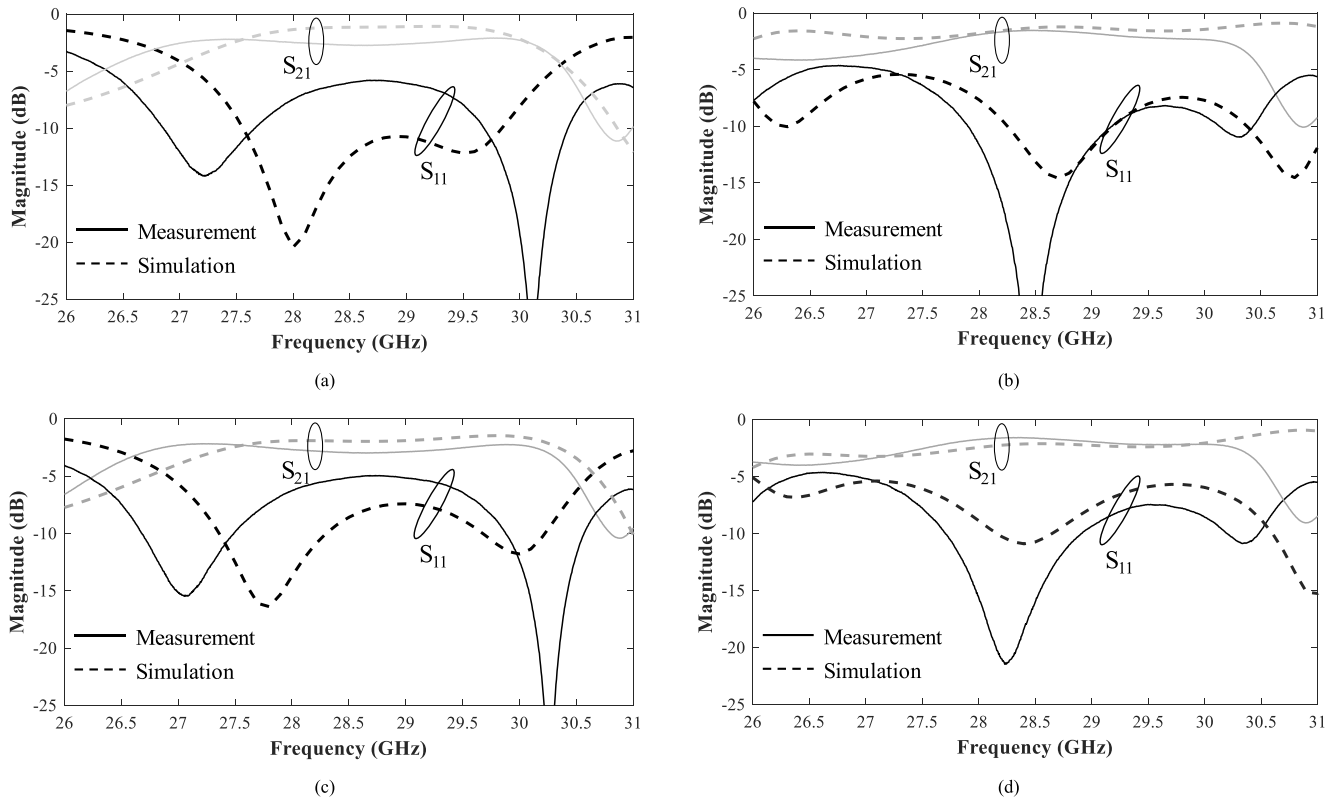


FIGURE 6. Simulated and measured reflection and transmission coefficients of the unit-cell in the four phase states: (a) UC000, (b) UC090, (c) UC180, and (d) UC270. The measured results have been obtained using the waveguide setup described in Section II.B and the simulations have been carried out using Ansys HFSS v2018.

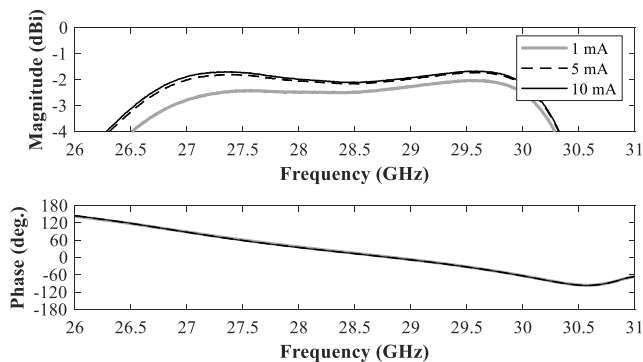


FIGURE 7. Measured transmission coefficients in amplitude and phase for UC000 as a function of the diode p-i-n bias current. Note that the measured phase responses are superposed.

B. IMPACT OF BIAS CURRENT

To highlight the tradeoff between unit-cell power consumption and insertion loss, the impact of the bias current on the unit-cell performance has also been investigated. Here, the bias current varies in the range 1-10 mA. The corresponding measured transmission coefficients of the UC000 are plotted in amplitude and phase in Fig. 7 for the bias current values 1, 5, and 10 mA.

The measured minimum insertion losses are provided in Table 2 for the four phase states. Their value increases by about 0.5 dB for a bias current of 1 mA (compared to 10 mA) while the total power consumption is reduced by a

TABLE 2. Measured minimum insertion loss of the 2-bit unit-cell as a function of the p-i-n diodes bias current.

I_{bias} (mA)	UC000	UC090	UC180	UC270
1	2.03 dB	1.87 dB	2.01 dB	1.95 dB
3	1.78 dB	1.54 dB	1.76 dB	1.63 dB
5	1.72 dB	1.46 dB	1.70 dB	1.56 dB
7	1.70 dB	1.41 dB	1.67 dB	1.51 dB
10	1.67 dB	1.39 dB	1.66 dB	1.48 dB

TABLE 3. Measured transmission phase at 29 GHz of the 2-bit unit-cell as a function of the p-i-n diodes bias current.

I_{bias} (mA)	UC000	UC090	UC180	UC270
1	174.4°	56.4°	-6.99°	-132.9°
3	173.7°	55.8°	-7.73°	-133.6°
5	173.6°	55.6°	-7.90°	-133.8°
7	173.5°	55.7°	-7.94°	-133.9
10	173.5°	55.6°	-7.91°	-133.9°

factor 10. The measured increase of insertion loss at 29 GHz for a bias current 1 mA (compared to 10 mA) is equal to 0.33, 0.45, 0.35 and 0.39 dB for UC090, UC180, and UC270, respectively.

To complete the analysis, the measured transmission phase at 29 GHz when the bias current varies in the range 1-10 mA is presented in Table 3. It is important to notice, that the

transmission phase response remains very stable on the full operation bandwidth as a function of the bias current value.

IV. CONCLUSION

A 2-bit electronically reconfigurable unit-cell for steerable transmitarray has been optimized, fabricated, and fully characterized in a waveguide measurement setup. Four p-n diodes have been integrated on the two radiating elements to control electronically the transmission phase with the required 90° phase-shift difference.

The unit-cell frequency response has been also studied experimentally as a function of the p-i-n diode forward bias current (from 1 to 10 mA). At 29 GHz the nominal transmission insertion loss measured with a bias current of 10 mA is in the range 1.39–1.67 dB. The 3-dB transmission phase bandwidth varies between 10.1% and 12.1%. The experimental results show an acceptable agreement when compared to full-wave electromagnetic simulations.

REFERENCES

- [1] S. V. Hum and J. Perruisseau-Carrier, "Reconfigurable reflectarrays and array lenses for dynamic antenna beam control: A review," *IEEE Trans. Antennas Propag.*, vol. 62, no. 1, pp. 183–198, Jan. 2014.
- [2] J. G. Nicholls and S. V. Hum, "Full-space electronic beam-steering transmitarray with integrated leaky-wave feed," *IEEE Trans. Antennas Propag.*, vol. 64, no. 8, pp. 3410–3422, Aug. 2016.
- [3] A. Clemente, M. Smierzchalski, M. Huchard, C. Barbier, and T. L. Nadan, "Characterization of a low-profile quad-feed based transmitarray antenna at V-band," in *Proc. 49th Eur. Microw. Conf. (EuMC)*, Paris, France, Oct. 2019, pp. 232–235.
- [4] A. R. Vilenskiy, M. N. Makurin, and C. Lee, "Phase distribution optimization for 1-bit transmitarrays with near-field coupling feeding technique," in *Proc. 14th Eur. Conf. Antennas Propag. (EuCAP)*, Copenhagen, Denmark, 2020, pp. 1–5.
- [5] J. R. Reis, R. F. S. Caldeirinha, A. Hammoudeh, and N. Copner, "Electronically reconfigurable FSS-inspired transmitarray for 2-D beamsteering," *IEEE Trans. Antennas Propag.*, vol. 65, no. 9, pp. 4880–4885, Sep. 2017.
- [6] J. Y. Lau and S. V. Hum, "A wideband reconfigurable transmitarray element," *IEEE Trans. Antennas Propag.*, vol. 60, no. 3, pp. 1303–1311, Mar. 2012.
- [7] J. R. Reis, M. Vala, and R. F. S. Caldeirinha, "Review paper on transmitarray antennas," *IEEE Access*, vol. 7, pp. 94171–94188, 2019.
- [8] M. Frank, F. Lurz, R. Weigel, and A. Koelpin, "Electronically reconfigurable 6×6 element transmitarray at K-band based on unit cells with continuous phase range," *IEEE Antennas Wireless Propag. Lett.*, vol. 18, no. 4, pp. 796–800, Apr. 2019.
- [9] C.-C. Cheng, B. Lakshminarayanan, and A. Abbaspour-Tamijani, "A programmable lens-array antenna with monolithically integrated MEMS switches," *IEEE Trans. Microw. Theory Techn.*, vol. 57, no. 8, pp. 1874–1884, Aug. 2009.
- [10] W. Pan, C. Huang, X. Ma, B. Jiang, and X. Luo, "A dual linearly polarized transmitarray element with 1-bit phase resolution in X-band," *IEEE Antennas Wireless Propag. Lett.*, vol. 14, pp. 167–170, 2015.
- [11] C. Huang, W. Pan, and X. Luo, "Low-loss circularly polarized transmitarray for beam steering application," *IEEE Trans. Antennas Propag.*, vol. 64, no. 10, pp. 4471–4476, Oct. 2016.
- [12] M. Wang, S. Xu, F. Yang, and M. Li, "Design and measurement of a 1-bit reconfigurable transmitarray with subwavelength H-shaped coupling slot elements," *IEEE Trans. Antennas Propag.*, vol. 67, no. 5, pp. 3500–3504, May 2019.
- [13] B. D. Nguyen and C. Pichot, "Unit-cell loaded with PIN diodes for 1-bit linearly polarized reconfigurable transmitarrays," *IEEE Antennas Wireless Propag. Lett.*, vol. 18, no. 1, pp. 98–102, Jan. 2019.
- [14] L. Di Palma, A. Clemente, L. Dussopt, R. Sauleau, P. Potier, and P. Pouliguen, "Circularly-polarized reconfigurable transmitarray in Ka-band with beam scanning and polarization switching capabilities," *IEEE Trans. Antennas Propag.*, vol. 65, no. 2, pp. 529–540, Feb. 2017.
- [15] F. Diaby, A. Clemente, R. Sauleau, K. T. Pham, and L. Dussopt, "2 bit reconfigurable unit-cell and electronically steerable transmitarray at Ka-band," *IEEE Trans. Antennas Propag.*, vol. 68, no. 6, pp. 5003–5008, Jun. 2020.
- [16] A. Clemente, L. Di Palma, F. Diaby, L. Dussopt, K. Pham, and R. Sauleau, "Electronically-steerable transmitarray antennas for Ka-band," in *Proc. 13th Eur. Conf. Antennas Propag. (EuCAP)*, Krakow, Poland, 2019, pp. 1–4.
- [17] F. Diaby, A. Clemente, L. Di Palma, L. Dussopt, K. Pham, E. Fourn, and R. Sauleau, "Design of a 2-bit unit-cell for electronically reconfigurable transmitarrays at Ka-band," in *Proc. 47th Eur. Radar Conf. (EURAD)*, Nuremberg, Germany, Oct. 2017, pp. 1321–1324.
- [18] L. Di Palma, A. Clemente, L. Dussopt, R. Sauleau, P. Potier, and P. Pouliguen, "1-bit reconfigurable unit cell for Ka-band transmitarrays," *IEEE Antennas Wireless Propag. Lett.*, vol. 15, pp. 560–563, 2016.
- [19] P. W. Hannan and M. A. Balfour, "Simulation of a phased-array antenna in waveguide," *IEEE Trans. Antennas Propag.*, vol. AP-13, no. 3, pp. 342–353, May 1965.



ANTONIO CLEMENTE (Senior Member, IEEE) received the B.S. and M.S. degrees in telecommunication engineering and remote sensing systems from the University of Siena, Italy, in 2006 and 2009, respectively, and the Ph.D. degree in signal processing and telecommunications from the University of Rennes 1, France, in 2012.

From October 2008 to May 2009, he realized his master thesis project at the Technical University of Denmark (DTU), Lyngby, Denmark, where he worked on spherical nearfield antenna measurements. His Ph.D. has been realized at CEA-Leti, Grenoble, France. In 2012, he joined the Research and Development Laboratory of Satimo Industries, Villebon-sur-Yvette, France. Since 2013, he has been a Research Engineer with CEA-Leti. He has authored or coauthored more than 100 articles in international journals and conferences, and received 12 patents. From 2016 to 2018, he has been the Technical Coordinator of the H2020 joint Europe and South Korea 5GCHAMPION project. He serves as a reviewer for the numerous IEEE and IET journals in the field of Microwave, Antennas and Propagation. His current research interests include fixed-beam and electronically reconfigurable transmitarray antennas, millimeter-wave and sub-THz antennas, antenna arrays, near-field focused systems, antenna modelling, miniature integrated antennas, antenna fundamental limitations, and near-field and far-field antenna measurements.

Dr. Clemente received the Young Scientist Award (First Prize) during the 15th International Symposium of Antenna Technology and Applied Electromagnetics (ANTEM 2012) and the Best Antenna Design and Applications Paper Award during the 13th European Conference on Antennas and Propagation (EuCAP 2109). He was a co-recipient of the Best Paper Award at JNM 2015 (19emes Journées Nationales Microondes) and the 2019 ETRI Journal Best Paper Award.



FATIMATA DIABY received the B.S. degree in physics from the University Joseph Fourier, Grenoble, France, in 2011, and the M.S. degree in microelectronics and telecommunication engineering from Polytech Marseille, France, in 2014. She is currently pursuing the Ph.D. degree with the Laboratory of Antenna Propagation and Inductive Coupling (LAPCI), CEA-Leti, Grenoble.

Her research interests include electronically reconfigurable transmitarray antennas and the development of numerical tools dedicated to the modeling and optimization of transmit arrays.

Dr. Diaby was a co-recipient of the Best Antenna Design and Applications Paper Award during the 13th European Conference on Antennas and Propagation (EuCAP 2109).



LUCA DI PALMA (Member, IEEE) was born in Rome, Italy, in 1987. He received the B.Sc. degree (*summa cum laude*) in electronics and the M.Sc. degree (*summa cum laude*) in telecommunication engineering from the University of Roma Tre, Rome, in 2009 and 2011, respectively, and the Ph.D. degree in signal processing and telecommunications from the University of Rennes 1, Rennes, France, in 2015.

From 2013 to 2015, he worked as a Research Assistant with CEA-Leti, Grenoble, France. Since 2016, he has been a Microwave and Antenna Engineer with Airbus Defence and Space in Italy. He has contributed to more than 40 articles and communications in revues and national and international conferences on antennas and microwave circuits. He serves as a Reviewer for the IEEE TRANSACTIONS ON ANTENNAS AND PROPAGATION, the IEEE ANTENNAS AND WIRELESS PROPAGATION LETTER, and IEEE ACCESS journals. His M.Sc. thesis project on metamaterials was awarded at the Marconi Junior Prize (Second Place), in 2012, Pontecchio Marconi, Italy. His research interests include metamaterials, wide-coverage antennas, phased arrays, reflector design, quasi-optic reconfigurable antennas, and planar and waveguide components at microwave and millimeter-wave frequencies with focus on satellite applications.

Dr. Di Palma received the Best Paper Award from the French National Conference on Microwaves (JNM 2015), Bordeaux, France, in June 2015. He was a co-recipient of the Best Antenna Design Paper Award at the European Conference on Antennas and Propagation (EuCAP 2019), Krakow, Poland, in April 2019.



LAURENT DUSSOPT (Senior Member, IEEE) received the M.S. degree in electrical engineering from the Ecole Normale Supérieure de Cachan, France, the Ph.D. degree in electrical engineering from the University of Nice-Sophia Antipolis, France, in 2000, and the Habilitation à Diriger des Recherches degree from University Joseph Fourier, Grenoble, France, in 2008.

He was a Research Fellow with the University of Michigan, Ann Arbor, from 2000 and 2002, where he developed reconfigurable microwave circuits and antennas based on RF-MEMS technology. Since 2003, he has been with CEA-Leti, France, as a Research Engineer and a Project Leader on advanced antenna systems for wireless communications at microwave and millimeter-wave frequencies. From 2013 to 2016, he has been a Chief Scientist of the Systems Division, CEA-Leti. Since 2016, he has been working on THz imaging systems with the Optics and Photonics Division, CEA-Leti. He is currently a Research Director of CEA-Leti. He has published more than 180 scientific articles in international journals and conferences, eight book chapters, and several patents; he has contributed to the technical program committees of several international conferences and the IEEE MTT-20 Technical Committee on wireless communications and organized several workshops in this field.

Dr. Dussopt received the Lavoisier Postdoctoral Fellowship from French Government, in 2000. He was a co-recipient of conference prizes at the IEEE RFIC'2002, ANTEM'2012, JNM'2015, and EuCAP'2019.



RONAN SAULEAU (Fellow, IEEE) received the degree in electrical engineering and radio communications from the Institut National des Sciences Appliquées, Rennes, France, in 1995, the Agrégation degree from the Ecole Normale Supérieure de Cachan, France, in 1996, and the Ph.D. degree in signal processing and telecommunications and the Habilitation à Diriger des Recherches degree from the University of Rennes 1, France, in 1999 and 2005, respectively.

He was an Assistant Professor and an Associate Professor with the University of Rennes 1, from September 2000 to November 2005, and from December 2005 to October 2009, respectively. He has been appointed as a Full Professor with the University of Rennes 1, since November 2009. He has been the Co-Director of the research Department Antenna and Microwave Devices, IETR, and the Deputy Director of IETR, until 2016. He is currently the Director of IETR. He has been involved in more than 45 research projects at the national and European levels and has co-supervised 20 post-doctoral fellows, 45 Ph.D. students, and 50 master students. He received 20 patents and is the author or coauthor of more than 220 journal articles and 480 publications in international conferences and workshops. He has shared the responsibility of the research activities on antennas at IETR in 2010 and 2011. His current research interests include numerical modeling (mainly FDTD), millimeter-wave printed and reconfigurable (MEMS) antennas, substrate integrated waveguide antennas, lens-based focusing devices, periodic and non-periodic structures (electromagnetic bandgap materials, metamaterials, reflectarrays, and transmitarrays), and biological effects of millimeter waves.

Prof. Sauleau has also been a member of the board of directors of EurAAP, since 2013. He received the 2004 ISAP Conference Young Researcher Scientist Fellowship, Japan, and the first Young Researcher Prize in Brittany, France, in 2001, for his research work on gain-enhanced Fabry-Perot antennas. In September 2007, he was elevated to junior member of the Institut Universitaire de France. He was awarded the Bronze medal by CNRS, in 2008. He was a co-recipient of several international conference awards with some of his students (International School of BioEM 2005, BEMS'2006, MRRS'2008, E-MRS'2011, BEMS'2011, IMS'2012, Antem'2012, BioEM'2015, ESA Workshop'2018, and EuCAP'2019). He has served as a Guest Editor for the IEEE ANTENNAS PROPAGATION special issue on Antennas and Propagation at mm and sub mm waves. He has served as a national delegate for COST VISTA. He has been national delegate for EurAAP, from 2013 to 2018.

...